Konya Mühendislik Bilimleri Dergisi, c. 13, s. 1, 74-97, 2025
Konya Journal of Engineering Sciences, v. 13, n. 1, 74-97, 2025
ISSN: 2667-8055 (Electronic)
DOI: 10.36306/konjes.1558191

CHARACTERIZATION OF EPOXY RESIN AND SILLE STONE POWDER BASED COMPOSITE MORTARS

[1,*] Ahmet Cihat ARI, [2] Mustafa TOSUN

[1] Yozgat Bozok University, Akdagmadeni Vocational School, Architecture and Urban Planning Department, Yozgat, TÜRKİYE
[2]-Konya Technical University, Architecture and Design Faculty, Architecture Department, Konya, TÜRKİYE
[1] a.cihat.ari@bozok.edu.tr, [2] mtosun@ktun.edu.tr

Highlights

- Mechanical properties of epoxy resin and Sille stone powder based composite mortars.
- Development of new restoration mortars.
- Physical and microstructure properties of composite mortars.

Graphical Abstract

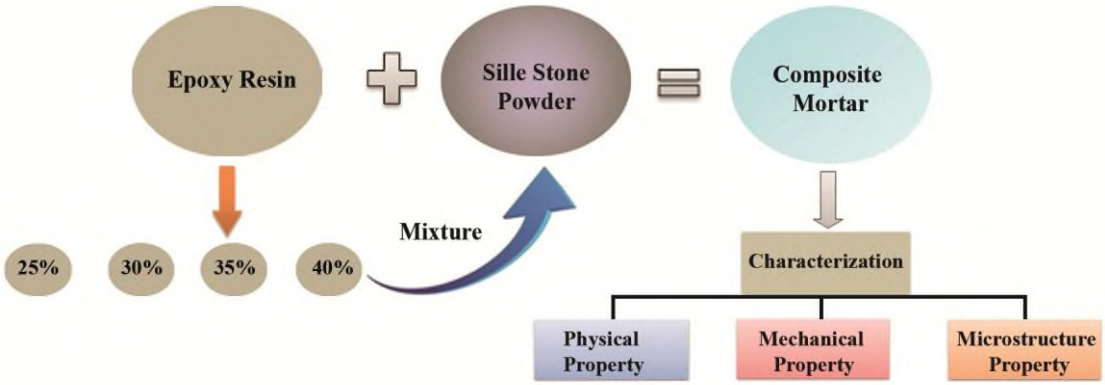

Schematic illustration of production epoxy resin and Sille stone powder based composite mortars

***Corresponding Author:** Ahmet Cihat ARI, a.cihat.ari@bozok.edu.tr

Konya Mühendislik Bilimleri Dergisi, c. 13, s. 1, 74-97, 2025
Konya Journal of Engineering Sciences, v. 13, n. 1, 74-97, 2025
ISSN: 2667-8055 (Electronic)
DOI: 10.36306/konjes.1558191

CHARACTERIZATION OF EPOXY RESIN AND SILLE STONE POWDER BASED COMPOSITE MORTARS

[1,*] Ahmet Cihat ARI, [2] Mustafa TOSUN

[1] *Yozgat Bozok University, Akdagmadeni Vocational School, Architecture and Urban Planning Department, Yozgat, TÜRKİYE*
[2] *Konya Technical University, Architecture and Design Faculty, Architecture Department, Konya, TÜRKİYE*
[1] a.cihat.ari@bozok.edu.tr, [2] mtosun@ktun.edu.tr

(Received: 30.09.2024; Accepted in Revised Form: 07.01.2025)

ABSTRACT: Sille stone, extracted from the Sille region of Konya (Türkiye) province, is an andesitic stone used in the construction of historical buildings. Sille stone is subject to deterioration due to long-term natural and environmental factors. Repair mortars are used to prevent damage to the stones used in the construction of historical buildings. In this study, Epoxy resin (ER)/Sille stone powder (SSP) composite mortars were produced for the restoration of historical buildings and the properties of these composite mortars were investigated. In the production of composite mortars were prepared by contributing SSP into epoxy resin in varied ratios such as 60-75% wt.%. When 60% SSP filler was added to the ER matrix, the compressive strength of the resulting composite increased by approximately 66% compared to neat ER. Moreover, an increase in mechanical strength and a decrease in water absorption were observed in composite mortars due to the increase in SSP. In conclusion, the high strength, low water absorption rate and pore properties of epoxy matrix composite mortars provide great potential for restoration applications of historical buildings constructed from Sille stone.

Keywords: *Characterization, Composite Mortar, Cultural Heritage, Sille Stone*

1. INTRODUCTION

Repair mortars are used in the restoration of cracks or missing damaged areas in the material used in the construction of cultural assets. While the repair mortars are being developed, it is important to ensure the harmony between the material properties of the historical artifact in terms of preserving the historical properties of the building. For this reason, it is necessary to determine the properties of the components such as binder and aggregate in the repair mortar and to carry out restoration studies according to these properties. Additionally, knowing the properties of repair mortars ensures the durability of the historical artifact and the restoration compatibility of the building [1]. The use of repair mortars, similar to the material used in the construction of the historical monument, in the restoration works prevents new damages that may occur due to freezing-thawing events, and this is beneficial for the protection of cultural assets. The compatibility of the repair mortars with the original material in the design is important in terms of providing maximum protection with the principle of minimum intervention in the restoration of the building [2]. For this reason, the compatibility of repair mortars with the original material contributes to the development of the restoration intervention strategy of the building. Moreover, the development of repair mortars helps repair specialists to restore the building to its original form.

The stone used in the construction of cultural assets was preferred because of its strength and durability compared to other masonry materials. However, factors such as weathering of the stone material due to environmental conditions, physical changes of the structure, changes in temperature and humidity cause deterioration in the material [3]. Cultural assets built of Sille stone in Konya have been damaged due to climatic and environmental factors. In particular, the fact that Sille stone has been used both in Roman, Seljuk and Ottoman civilizations throughout the history in Konya and in the construction of today's buildings necessitates taking precautions against the deterioration problems that

***Corresponding Author:** Ahmet Cihat ARI, a.cihat.ari@bozok.edu.tr

occur in these stones [4]. Many researchers have investigated the deterioration of Sille stone [4-9]. In the study conducted by Ozdemir [8], it was determined that cultural assets made of Sille stone in Konya are effective in the formation of moisture on the facade surfaces due to the porosity of the stone and the high amount of water absorption. In the study conducted by Fener and İnce [4] determined the mechanical and wear properties of freeze-thaw deterioration processes in Sille stone due to atmospheric effects. In the review made in the literature, the solution of the damages on the facade surfaces caused by the high water absorption amount in Sille stone was not mentioned. Additionally, no study has been published on the development of repair mortar to be used in the restoration of Sille stone.

Sille stone is cut to certain sizes before it is used in buildings and wastes are generated during this cutting process [10]. For this reason, the production of composite materials by evaluating waste products contributes to both the reduction of costs and the protection of the environment and nature. Regarding the production of composite materials from Sille stone powder, Öztürk, et al. [10] conducted a study on the use of floor tiles in their article. In the study, it has been concluded that Sille stone has a positive contribution to heat resistance and high strength floor tile products. Except for this study, no study has been found in the literature on the production of composite materials using Sille stone powder.

In the literature, studies have been carried out on the development of repair mortar, lime-based mortar [11], lime mortar with pozzolanic additives (brick powder) [12], organic-added lime mortar (brass) [13], industrial waste additive alkali active mortar (fly ash and blast furnace slag) [14] and polymer added mortar (epoxy) [15, 16]. Epoxy resins are used in the restoration of various stone materials due to their resistance to water, good adhesion to the substrate, and mechanical and abrasion resistance. For instance, Tesser, et al. [17], investigated the physicochemical properties of mortars produced with epoxy binders for use in the repair of marble and limestone. In the same study, it was determined that mortars produced with epoxy binders were resistant to biological deterioration in addition to providing structural stone reinforcement of monuments. In the research conducted by Alonso-Villar, et al. [18], the properties of mortars produced with and without the addition of micronized silica to epoxy and acrylic resins in the repair of historical buildings constructed from granite stone were investigated. It was determined that mortars produced by adding micronized silica significantly reduce the water absorption rate of the stone. In another study conducted by Roig-Salom, et al. [19], the properties of mortars produced with epoxy binders in the restoration of historical marble fountains were investigated. It was determined that mortars produced with epoxy binder are resistant to biological attacks and have similar mechanical behavior to natural marble. In all these studies, it was reported that mortars produced with epoxy binders have great potential in the restoration of historical buildings, in combining broken pieces of stones and in closing cracks and surface cavities. Additionally, it was stated in the literature that the properties of polymer-binding composite mortars should be examined before the restoration of historical buildings because stone types have different properties and different structural behaviors can occur as a result of the chemical reaction between the polymer material and the stone. To our knowledge, while the mechanical and physical properties of Sille stone are the subject of further research, no research has been conducted to date on the development of repair mortars for use in the restoration of historical buildings using Sille stone. This study investigates the properties of Sille stone powder and epoxy binder mortars for the restoration of historical buildings for the first time and fills the existing knowledge gap caused by the lack of sufficient number of studies in the literature on the use of polymer binder materials as repair mortars.

In this study, the development and characterization of Sille stone powder–epoxy matrix repair mortar was investigated for its usability in the restoration of cultural assets in Konya. Additionally, the physical and mechanical properties of Sille stone powder added epoxy matrix composite mortar were investigated. However, in the study, economical and high-strength composite mortar was produced by using Sille stone powder wastes for the restoration of cultural assets.

2. MATERIAL AND METHODS

In this chapter, the materials used in the study and their properties are explained. Additionally,

information is given about the methods applied in the characterization of composite sample samples produced from these materials.

2.1. Materials Used in Experiment Studies

Information about the materials used in the test studies, their locations and some properties of these materials are given below.

2.1.1. Sille Stone Powder (SSP)

The SSP used for the production of composite mortar was taken from a quarry in Sille region of Konya province. Since Sille stones were shaped in various sizes before being used as building materials, stone powders were collected from the quarry for experimental studies (Figure 1). Sieve analysis was performed for particle size distribution of SSP taken from the quarry. Stone powder was sieved using a sieve device (Retsch AS 200) and sieves of different sizes (63, 150, 250, 500, 1000, 2000 and 4000 μm). Each of the sieve set apparatus was placed with 100 gr SSP and then shaking was done for 10 minutes. At the end of this process, the powder remaining in each sieve was weighed and recorded. In the particle size distribution of SSP, approximately half of the particles are below 63 μm, while less than 10% of the particles are larger than 500 μm (Figure 2). Some features of the SSP used in the experimental study are given in Table 1. The chemical content of SSP is given in Table 2. It was determined that the chemical content of SSP was highest as SiO_2 66.67% and Al_2O_3 13.24%.

Figure 1. Photograph of the SSP used in the study

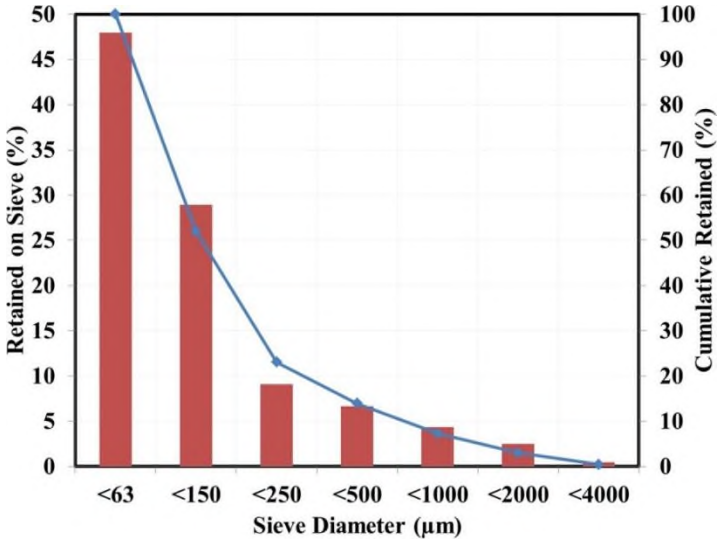

Figure 2. Particle size distribution of SSP [20]

Table 1. Some features of SSP used in this research [8, 21]

Sille stone powder (SSP)	Density (g.cm^{-3} at 20 °C):	2.26 – 2.35
	Water absorption (%, at 23 °C):	3.9
	Melting point (°C):	2000

Table 2. Chemical content of the SSP [22]

Content of the SSP	**SiO_2**	**Al_2O_3**	**K_2O**	**Na_2O**	**MgO**	**CaO**	**Fe_2O_3**	**TiO_2**	**ZrO_2**
%	66.67	13.24	4.11	4.94	1.09	5.07	3.66	0.52	0.39

2.1.2. Epoxy Resin (ER)

The ER was used as the matrix material within the scope of the study. Bisphenol-A type epoxy resin and hardener, cycloaliphatic polyamine BRTR Kimya A.Ş. (Türkiye) was purchased from the company. Epoxy and hardener have transparent color, glossy appearance, the mixture is cured for 12 hours at 25°C, mechanical strength is completed in 7 days, and density of 1.10 g/cm^3.

2.2. Method

The preparation method of the composite samples and the information about the tests performed on these samples are explained below.

2.2.1. Preparation of Composite Sample

Within the scope of this study, the SSP composite sample with neat epoxy resin and epoxy matrix was produced. Neat ER sample was obtained by adding a 5:3 wt. cycloaliphatic polyamine hardener to the neat ER, and the mixture was stirred for 3 minutes. For the production of SSP composite sample with epoxy matrix; each mixture in these composites was added to neat ER at 60 %, 65 %, 70% and 75% weight ratios and mixed for 3 minutes. Then, the cycloaliphatic polyamine hardener was added to the composite mixtures in a ratio of 5:3 by weight. Each of the obtained composite samples was mixed for 3 minutes (Table 3 and Figure 3). Composite samples were produced using the traditional hand lay-up

technique. Additionally, due to the high viscosity of the mixture, it was mixed manually without using a mechanical mixer. The reason for choosing this method is that it uses less equipment, does not require any heat treatment, and allows for fast and serial production under application conditions. The composite mortars that were mixed were cast in molds in accordance with ASTM standard and all the composite mortars produced were dried in these molds at room temperature for 24 hours.

Table 3. The abbreviations and ingredients of composite mortars

Composite mortars' abbreviations	Combination ratio of resin type/SSP
ER	100:0
ER/SSP-1	40:60
ER/SSP-2	35:65
ER/SSP-3	30:70
ER/SSP-4	25:75

Figure 3. (a) Photograph of the composite sample produced within the scope of the study, (b) Photograph of the Sille stone

2.2.2. Experiments on Composite Mortar

Within the scope of this study, experiments were carried out to determine the physical, chemical, mechanical and microstructural properties of the produced composite mortars. Compression tests were carried out to determine the strength and durability of composite mortars obtained from the epoxy resin mixture of SSP. Flexural test was also performed to determine the resistance of composite mortars against flexural under load. Since the adhesion force between the wall and the mortar causes mechanical tensile stresses in the mortars, tensile tests were carried out to determine the resistance of the composite mortars against mechanical tensile stresses. Depending on the increase in the SSP ratio in composite mortars, hardness tests were performed to determine the hardness and durability of the material. Water absorption test and void content were performed to determine the water resistance of composite mortars and the amount of water absorption of the material. SEM-EDS analysis was performed to determine the morphology of composite mortars and the changes that occur in the material due to increasing the SSP ratio in the composite material. FTIR analyses of composite mortars were performed to determine the properties of molecular bonds formed by the chemical interaction between epoxy resin and stone powder. All these experiments were carried out to evaluate whether the composite mortars produced within the scope of the study are suitable for use in restoration applications. One composite sample each was used for void content, SEM-EDS and FTIR analyses. Five composite samples each were used in the water absorption test, compression test, flexural test, tensile test and hardness test.

2.2.2.1. Void Content

The amount of space and pore size of the repair mortar material used in the restoration of historical monuments affect the water absorption rate of the building. The presence of high water absorption causes freezing-thawing events in the material and causes damage to the structures. In order to prevent structural damage caused by atmospheric effects, it is necessary to determine the gap of the mortar

material used in the restoration of historical monuments. Within the scope of the research, the pore amount and size of the repair mortar material produced was determined by the pore size and the mercury porosimetry method (Micromeritics - Autopore 4) with the help of the formula in the ASTM-D2734 standard [23]. The mercury porosimetry method is used to determine the pore size and pore size distribution in the material. It is ensured that fine pores of mercury penetrate the material with sufficient pressure. In the measurement of the pore size of the material, it is calculated by decreasing the amount of mercury with the applied pressure [24].

2.2.2.2. Water Absorption Test

The amount of water absorbed by the samples was determined by the water absorption test. In the water absorption test, the dry weights of the samples were measured at room temperature (23°C) on a precision balance with an accuracy of 0.001 g, then the samples were placed in containers filled with pure distilled water. After the samples were kept for 24 hours, dry weight differences were determined on a precision balance with 0.001 g precision. The water absorption percentages of the samples were calculated using the formula given in the standard in ASTM-D570 [25].

2.2.2.3. Flexural Test

Flexural test was done with SHIMADZU AGS-X device and samples were prepared in 4x13x165 mm molds. Additionally, 5 samples were produced for each type of composite samples and a force of 0.2mm/min was applied to these samples. In this experiment, the sample was placed on the supports horizontally in the device and the force values formed as a result of the deflection value in the middle of the samples were recorded. In the flexural test, both the die dimensions in the preparation of the samples and the force values of the samples were calculated according to the ASTM-D790 standard [26]. Moreover, the standard deviation value in the force values of the 5 samples measured for the force values of each type of composite in the flexural test was calculated.

2.2.2.4. Compression Test

In the compression test, the samples were prepared in 20x20x20 mm molds. The preparation of these samples was made according to the ASTM-D695 standard. SHIMADZU AGS-X device was used in the compressive strength test and the force velocity value was applied to the samples at 0.5mm/min. Compressive strength values were calculated with the help of the formula given in the ASTM-D695 standard [27]. Additionally, 5 samples were produced for each type of composite sample during these tests and the standard deviation in the compression strength values of the samples was calculated.

2.2.2.5. Tensile Test

It was aimed to determine the strength of the composite mortar against mechanical tensile forces by performing the tensile test. For this purpose, samples for the test were prepared in 19x115x4 mm molds according to ASTM-D638 standard. Moreover, the tensile test was performed with the SHIMADZU AGS-X device and the tensile force of the device was applied to the samples at a speed of 0.2mm/min. The specimens were placed at the lower and upper points of the device, and the deformations of the specimens and the maximum force values at the moment of rupture were recorded against the force applied in these two directions. The calculations in these measurements were made with the help of the formulas specified in the ASTM-D638 standard [28]. Additionally, the standard deviation in the force values of the 5 samples measured for the force values of each type of composite in the tensile test was calculated.

2.2.2.6. Hardness Test

Since different amounts of stone powder were added to the samples and the strength properties of the samples changed according to this stone powder, the hardness test was carried out. Hardness measurements of composite samples were made according to Shore D hardness measuring device and ASTM-D2240 standard. The plunge tip in the hardness measuring device was immersed in the samples, and the amount of depth formed in the sample and the hardness values of the composites were calculated. Moreover, the immersion tip of the device was immersed into the hardness value of the composites five times for each sample type and measurements were made and the standard deviation in the hardness values of the samples was calculated accordingly. Calculation of the hardness values in this experiment was made using the formulas in the ASTM-D2240 standard [29].

2.2.2.7. Scanning Electron Microscope-Energy Dispersive X-Ray Spectroscopy (SEM-EDS)

The morphological features of the samples were determined by Hitachi–SU 1510 SEM-EDS device. With the SEM device, the deformations and structural changes that occurred due to the increase of Sille stone powder in the composites were determined by surface scanning. The elements in the samples were determined by EDS analysis.

2.2.2.8. Fourier Transform Infrared Spectroscopy (FTIR)

FTIR analysis was performed to determine the properties of molecular bonds in the samples. FTIR analysis Thermo Scientific – Nicolet iS20 device was used. Infrared rays were sent to the samples with the FTIR device. Then, the wave energies formed in the vibrations of the molecular bonds during the absorption of infrared light in the samples were determined. FTIR analysis has an important place in the design of new products and in ensuring the quality control of the material. For this reason, the microstructure properties of the material were determined by performing FTIR analysis of the composite mortar.

3. RESULTS AND DISCUSSION

3.1. Void Content

Void content of ER/SSP samples, test result data are given in Table 4, Figure 4 and Figure 5. The pore size distribution of the samples showed a multi-peak distribution, while the pore size ranged between 0.01-300 μm. The density of the samples with pores was determined to be 0.005-0.25 mL/g. Additionally, the density of the samples with pores, the most significant peak was seen around 0.005 mL/g.

Table 4. Void determination test data of ER/SSP composites

Pore properties	ER/SSP-1	ER/SSP-2	ER/SSP-3	ER/SSP-4
Total Intrusion Volume (mL/g)	0.0409	0.0658	0.0488	0.0388
Total Pore Area (m^2/g)	5.850	15.846	15.139	11.657
Median Pore Diameter (Volume) (μm)	17.1643	0.0186	0.0126	0.0125
Median Pore Diameter (Area) (μm)	0.0081	0.0093	0.0077	0.0076
Average Pore Diameter (4V/A) (μm)	0.0280	0.0166	0.0129	0.0133
Bulk Density at 0.55 psia (g/mL)	1.6171	1.5740	1.6659	1.7479
Apparent (skeletal) Density (g/mL)	1.7316	1.7560	1.8133	1.8751
Porosity (%)	6.6139	10.3617	8.1293	6.7863
Stem Volume Used (%)	5	7	6	6

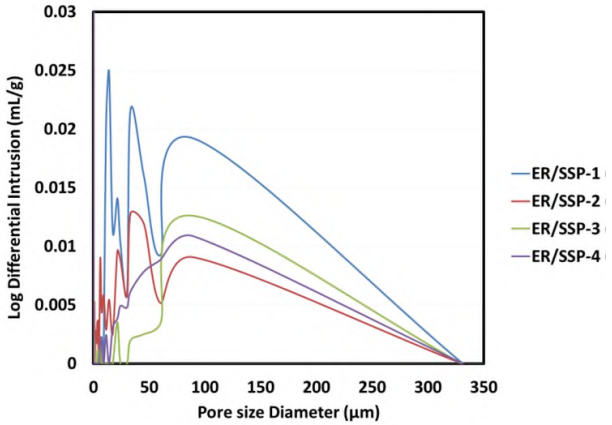

Figure 4. Void determination test result graph of ER/SSP composites

When the porosity ratios of ER/SSP composites are examined, the amount of voids decreases depending on the increase in the amount of SSP in all composites except ER/SSP-2 composite. According to the graph in Figure 5, it is seen that the porosity ratio of the ER/SSP-2 composite sample is higher than the porosity ratio of all other composites. The increase in the amount of voids in the material causes an increase in the water absorption rate. This situation causes deformations in the interior and exterior of the building such as humidity, blooming and rotting. The fact that the void ratio of the ER/SSP-4 sample developed within the scope of the study is the lowest, may help to reduce the damage caused by water absorption in the structure. Moreover, the use of this composite in the restoration of cultural assets may contribute to the long-term preservation of the structure.

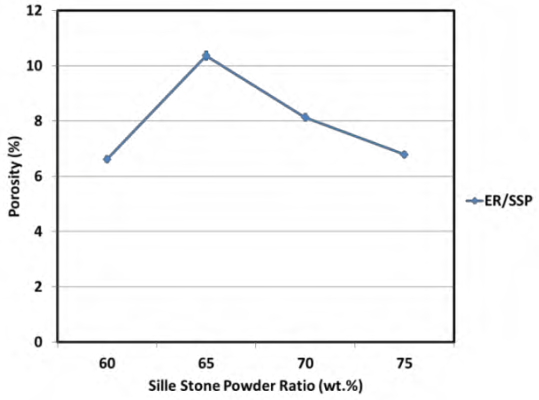

Figure 5. Graph of porosity (%) values of ER/SSP composites

In the study conducted by Lanas and Alvarez-Galindo [30] determined that the pore ratios of lime-based mortars ranged from 16.51% to 30.63%. In the study conducted by Török and Szemerey-Kiss [31] found that the pore ratios of limestones and portland pozzolanic cement repair mortars vary between 22.5% and 39.7%. In the study conducted by Zheng, et al. [32] showed in their study that the porosity ratios of epoxy resin-added cement-based mortar ranged from 5.19% to 14.46%. According to the studies in the literature, adding epoxy to the mortars reduces the pore rate. ER/SSP of composites the porosity varies between 6.61% and 10.36%, and a lower pore ratio than restoration mortars has been obtained in the literature. Additionally, this composite mortar gave a pore ratio comparable to epoxy resin-added mortars in the literature.

3.2. Water Absorption Test

The water absorption test of ER/SSP composites and Sille stone is given in Table 5 and the

comparison chart is given in Figure 6. According to the data in Table 5, it is seen that the water absorption rate of ER/SSP composites is lower than that of Sille stone. Moreover, in ER/SSP composites, the water absorption rate decreases due to the increase in the amount of Sille stone powder. It has been determined that the water absorption rate of the ER/SSP-4 composite has the lowest rate compared to all other composites. According to this test result, the fact that the composites are affected by water in the use of restoration repair mortar, and that it is less than Sille stone, prevents the deterioration of the structure caused by water. However, in the restoration of cultural assets, the low water absorption rate of the composite mortar prevents the damage caused during the freeze-thaw process due to atmospheric effects and the structure is preserved for a longer period of time.

Table 5. Water absorption test data of Sille stone and ER/SSP composites

Samples' ID	Composition Ratio (wt.%)	Water Absorption of Sille Stone and ER/SSP Composites (%)
ER/SSP-1	40:60	0.236
ER/SSP-2	35:65	0.181
ER/SSP-3	30:70	0.082
ER/SSP-4	25:75	0.070
Sille Stone	0:100	3.968

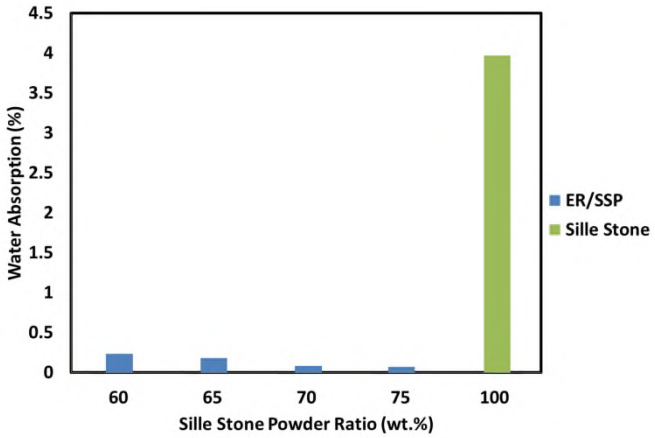

Figure 6. Graph of water absorption rate values of Sille stone and ER/SSP composites

In the study conducted by Korat, et al. [33] determined that the water absorption rate for tuff ranged from 8.0% to 8.3%, and the water absorption rate of mortars at atmospheric pressure ranged from 14.5% to 22.8%. In the study conducted by Alves, et al. [15] found that the water absorption data of epoxy polymer pozzolanic cement, white cement matrices and composites made with steatite rock powder vary between 0.27% and 13.72%. In the study conducted by Rahman and Islam [34] investigated the characterization of mortars made of epoxy resin and portland cement matrices with different proportions of sand. They observed that the water absorption rate of the epoxy matrix mortar was lower than the other matrix and the water absorption coefficient decreased due to the increase in the sand content. The ER/SSP composites have a water absorption rate between 0.07% and 0.236%, and this composite mortar has a lower water absorption rate than the restoration mortars in the literature. Moreover, the decrease in the water absorption coefficient of the composites due to the increase in stone powder shows that it is in good agreement with the literature.

3.3. Flexural Test

Flexural test results of ER/SSP composites are given in Table 6 and Figure 7. According to the data in Table 6, the flexural strength value of ER/SSP composites is between 20.11 MPa and 24.45 MPa. Moreover, it was determined that ER/SSP-4 composite had the highest strength value compared to other

composites. As seen in Figure 7, the reason for the decrease in the strength value of the composite from 60% to 65% by weight of SSP can be attributed to the agglomeration that occurs as a result of the interaction between the stone powder and the epoxy matrix. Agglomeration causes a decrease in the adherence between the epoxy matrix and the stone powder, and a decrease in the attraction force of the molecule in the stone powder. When these results are compared with the results of void determination; The fact that ER/SSP-2 composite has a higher porosity rate than other composites causes a decrease in strength. Moreover, the high amount of filling ensures that the void surface areas in the composite material are reduced. However, when the SSP is increased from 65% to 75% by weight, the strength value of the composite increases. Similar result is also seen in the study conducted by Rajput, et al. [35], in the flexural strength test of Kota stone powder as filler material in epoxy matrix. It was stated that there is an increase in flexural strength due to the higher surface hardness of stone particles compared to epoxy polymer. In the study conducted by Karthikeyan, et al. [36], in the flexural strength test of composites produced with marble powder and tamarind shell powder in epoxy matrix, it was found that the flexural strength increased due to the strengthening of the interface attraction in the composition when the ratio of epoxy resin was reduced. In the study conducted by Gomes, et al. [37], in the flexural strength test of composites produced with quarry powder (Brazil) and brick powder in the epoxy matrix, it was determined that the reduction of porosity in the composite material by homogeneously spreading the stone powder in the epoxy matrix increased the flexural strength. Therefore, as stated in literature studies, the decrease in porosity in the composite material by spreading the stone powder homogeneously in the epoxy matrix, the high surface hardness of the stone powder compared to the epoxy polymer and the strengthening of the interface attraction in its composition are the main reasons for the increase in the strength value of the composite.

Table 6. Flexural strength of ER/SSP composites

Samples' ID	Composition Ratio (wt.%)	Flexural Strength of ER/SSP Composites (MPa)
ER/SSP-1	40:60	21.12±1.38
ER/SSP-2	35:65	20.11±1.67
ER/SSP-3	30:70	23.28±2.02
ER/SSP-4	25:75	24.45±1.44

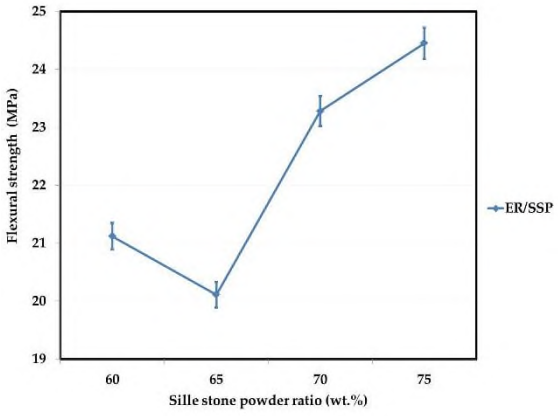

Figure 7. Flexural test result graph of ER/SSP composites

When the flexural test results of restoration mortars are examined in the literature, it varies between 0.07 MPa and 1.5 MPa in some studies [12, 30, 38, 39]. According to the studies in the literature, adding epoxy to the mortars increases the flexural strength [35, 40].

3.4. Compression Test

Compression test results of ER and ER/SSP composites are given in Table 7 and Figure 8. According to the data in Table 7, the strength value of ER/SSP composites is between 42.90 MPa and 52.36 MPa. Moreover, according to the compression test result, it was determined that the strength value of ER/SSP composites was higher than the strength value of neat ER (Figure 8). However, with the addition of 60% SSP filler to the ER matrix, its strength increased by 66% compared to neat ER. When the amount of SSP was increased from 60% to 70% by weight, the strength value of the composite decreased. The formation of agglomeration in the intermediate phase between the stone powder and the epoxy matrix causes a decrease in the adhesion strength of the matrix and a decrease in the strength of the composite. Nevertheless, when the amount of SSP was increased from 70% to 75% by weight, the stone powder was homogeneously dispersed in the epoxy matrix, and the decrease in the porosity ratio increased the strength value of the composite. When this result is compared with the flexural test result, the strength value of the composites gives similar results.

Table 7. Compressive strength of ER and ER/SSP composites

Samples' ID	Composition Ratio (wt.%)	Compressive Strength of ER/SSP Composites (MPa)
ER	100:0	28.31±2.34
ER/SSP-1	40:60	47.00±1.51
ER/SSP-2	35:65	45.11±0.47
ER/SSP-3	30:70	42.90±1.44
ER/SSP-4	25:75	52.36±1.78

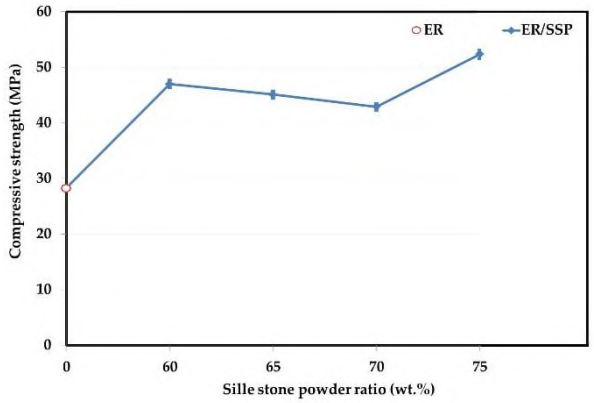

Figure 8. Compression test result graph of ER/SSP composites

When the compression test results related to the restoration mortars are examined in the literature, it varies between 0.3 MPa and 16 MPa in some studies [11, 12, 38, 39, 41] . In the study conducted by Kekeç [42] determined the compressive strength of Sille stone as 29.22 MPa. Moreover, in the literature, the addition of epoxy materials to improve the mechanical properties of repair mortars has contributed to the increase in the compressive strength of repair mortars [15, 34].

3.5. Tensile Test

The tensile test results of the ER/SSP composite are given in Table 8 and Figure 9. As shown in Table 8 and Figure 9, the tensile strength of ER/SSP composites is between 24.81 MPa and 27.30 MPa. Moreover, it was determined that ER/SSP-2 composite had the highest tensile value compared to other composites. When the amount of stone powder is increased from 60% to 65% by weight, an increase in tensile strength is observed, while a decrease in tensile strength is observed when the amount of stone

powder is increased from 65% to 70% by weight. While the filling loading strength of the composite material is increased to a certain extent, the filling loading causes a decrease in the adhesion force between the composite component when the ratio limit of the load is exceeded. Due to the non-homogeneous dispersed components of the composite in tensile strength, it leads to a decrease in its strength [40]. These results seem to be in agreement when compared with other results of mechanical property tests.

The ER/SSP-4 tensile test, which is another mixture obtained from the composite material, was carried out. These samples were prepared according to ASTM D638. ER/SSP-4 composite specimens could not be measured because they broke when their jaws were attached to the tensile testing machine. The main reasons for not measuring the ER/SSP-4 composite are the decrease in the bond strength between the stone powder and the epoxy matrix and the insufficient cure of the mixture during the production phase of the composite material [43, 44].

Table 8. Tensile strength of ER/SSP composites

Samples' ID	Composition Ratio (wt.%)	Tensile Strength of ER/SSP Composites (MPa)
ER/SSP-1	40:60	27.22±1.70
ER/SSP-2	35:65	27.30±1.45
ER/SSP-3	30:70	24.81±2.24

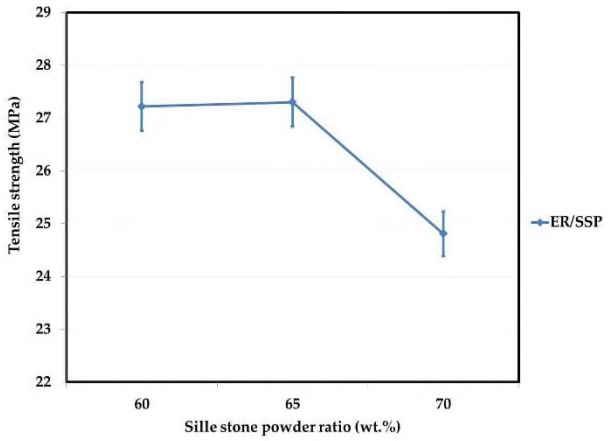

Figure 9. Tensile test result graph of ER/SSP composites

When the tensile test results of restoration mortars are examined in the literature, it varies between 2.5 MPa and 18 MPa in some studies [45-48]. According to the studies in the literature, adding epoxy to the mortars increases the tensile strength [45, 46, 48].

3.6. Hardness Test

The hardness test results of the ER/SSP composite are given in Table 9 and Figure 10. As seen in Table 9 and Figure 10, the hardness value of ER/SSP-4 composite is higher than the hardness value of all other composites. Moreover, an increase in the hardness value of the composite was observed when the amount of SSP was increased from 65% to 75% by weight. To explain the factor affecting this situation, the hardness of inorganic fillers can be attributed to the higher hardness of organic fillers [49]. Adding harder stone powder to the epoxy matrix can increase the hardness of the composite.

According to the data in Table 9 and Figure 10, it is seen that the hardness value of the ER/SSP-2 composite is lower than the other composites. It is seen that this result is compatible with the results of the void determination and other mechanical tests of the composite. As the void test result of ER/SSP-2 composite is explained, the fact that the porosity ratio is higher than the porosity ratio of other

composites causes a decrease in the hardness and strength of this composite. The increase in porosity and the amount of pores between the filler and the matrix creates agglomeration. This agglomeration leads to a decrease in the adhesion strength between the filler and the matrix, and a decrease in the strength of the composite material [50].

Table 9. Hardness test values of ER/SSP composites

Samples' ID	Composition Ratio (wt.%)	Shore-D Hardness Value of ER/SSP Composites
ER/SSP-1	40:60	81.4±0.5
ER/SSP-2	35:65	79.4±1.0
ER/SSP-3	30:70	81.2±1.0
ER/SSP-4	25:75	82.6±1.7

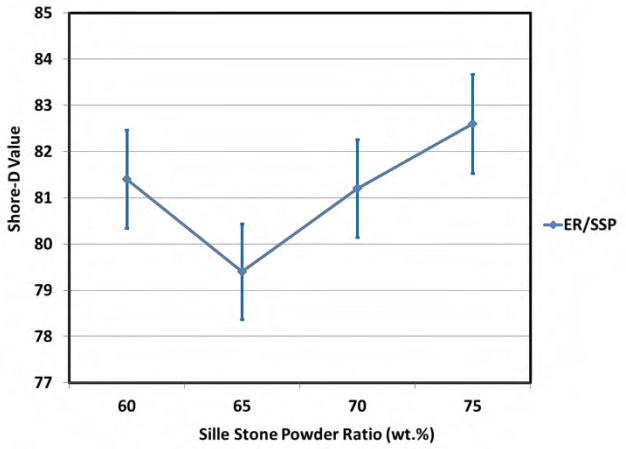

Figure 10. Shore-D hardness test result graph of ER/SSP composites

3.7. Scanning Electron Microscope-Energy Dispersive X-Ray Spectroscopy (SEM-EDS)

Figure 11 shows the SEM image of the ER/SSP composite taken at 500 μm magnification. Figure 11a shows that neat epoxy has a smooth surface texture. However, adding the amount of SSP to the epoxy matrix causes the composite material to form a rough and hollow structure (Figure 11b-11e). This structural change contributes to the improvement of the strength of the composite material. The less porous structure of the ER/SSP-4 composite compared to other composites is effective in its high strength as observed in the mechanical test results (Figure 11b-11e). However, stone powder loading fills the fine voids in the composite material and reduces the porosity rate. This shows that the bond strength between the epoxy matrix and the stone powder is strong (Figure 11e).

In Figure 11b and Figure 11c, the SEM image of ER/SSP composites shows agglomeration between the epoxy matrix and the stone powder on the surface. This agglomeration causes a decrease in the strength of the composite, as observed in the mechanical test results of the composite material. Moreover, the agglomerations occurring in the composite material prevent the reduction of the bond strength between the matrix and the stone powder and the homogeneous distribution of the stone powder particles on the matrix surface. This shows that the bond strength of the epoxy matrix decreases and the bond strength between the epoxy matrix and the stone powder are weak.

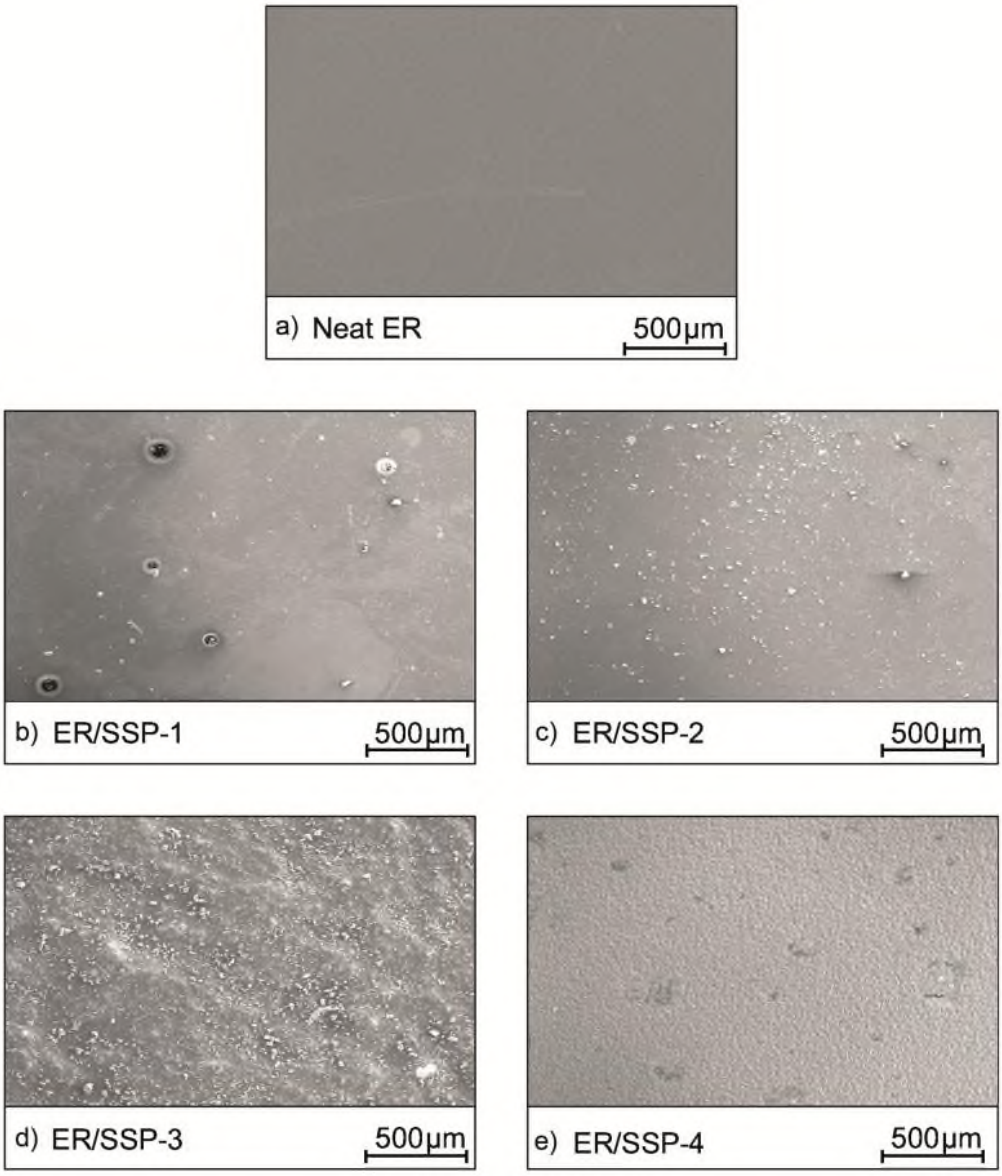

Figure 11. SEM image of ER/SSP composite

EDS analysis of ER/SSP-1 composite is given in Figure 12. When the map distribution of the elements in Figure 12 is examined, it is seen that it is the most dense carbon element. Moreover, the densities and distribution map of other elements in the ER/SSP-1 composite are oxygen, silicon, aluminum, potassium, iron, calcium, sodium and magnesium, respectively (Figure 12b-12j). It shows that the carbon and oxygen elements belong to the epoxy matrix. However, due to the carbonation of some of the compounds in Sille stone, the carbon element is also found in the stone powder. Oxygen and other elements are also present in the compounds of stone powder. According to the result of the EDS analysis of the ER/SSP-1 composite, it is observed that the epoxy matrix covers all the stone powder, and the stone powder is homogeneously dispersed into the epoxy matrix (Figure 12a-12k).

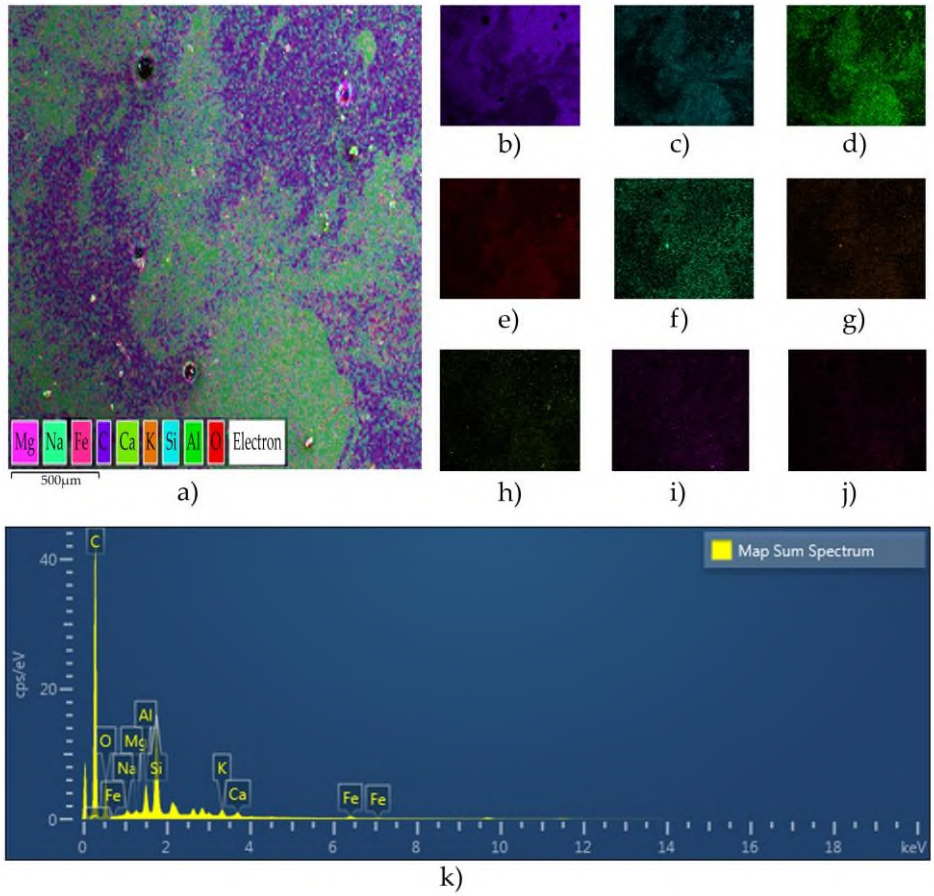

Figure 12. a) Elemental analysis and distribution map of ER/SSP-1 composite, b) Distribution of carbon element in ER/SSP-1 composite, c) Distribution of silicon element in ER/SSP-1 composite, d) Distribution of aluminum element in ER/SSP-1, e) Distribution of oxygen element in ER/SSP-1 composite, f) Distribution of sodium element in ER/SSP-1 composite, g) Distribution of potassium element in ER/SSP-1 composite, h) Distribution of calcium element in ER/SSP-1 composite, i) Distribution of magnesium element in ER/SSP-1 composite, j) Distribution of iron element in ER/SSP-1 composite, k) EDS analysis in ER/SSP-1 composite

EDS analysis of ER/SSP-2 composite is given in Figure 13. When the map distribution of the elements in Figure 13 is examined, it is seen that it is the most dense carbon element. Moreover, the densities and distribution map of the other elements in the ER/SSP-2 composite are oxygen, silicon, aluminum, potassium, iron, calcium, sodium and magnesium, respectively (Figure 13b-13j). It shows that the carbon and oxygen elements belong to the epoxy matrix. However, due to the carbonation of some of the compounds in Sille stone, the carbon element is also found in the stone powder. Oxygen and other elements are also present in the compounds of stone powder. ER/SSP-2 composite shows an increase in silicon element compared to ER/SSP-1. However, the oxygen element in ER/SSP-2 composite decreases compared to ER/SSP-1. This is due to an increase in the amount of stone powder and a decrease in the epoxy matrix. According to the result of the EDS analysis of the ER/SSP-2 composite, it prevents the homogeneous distribution of the elements due to the agglomeration that occurs between the epoxy matrix and the stone powder (Figure 13a-13k).

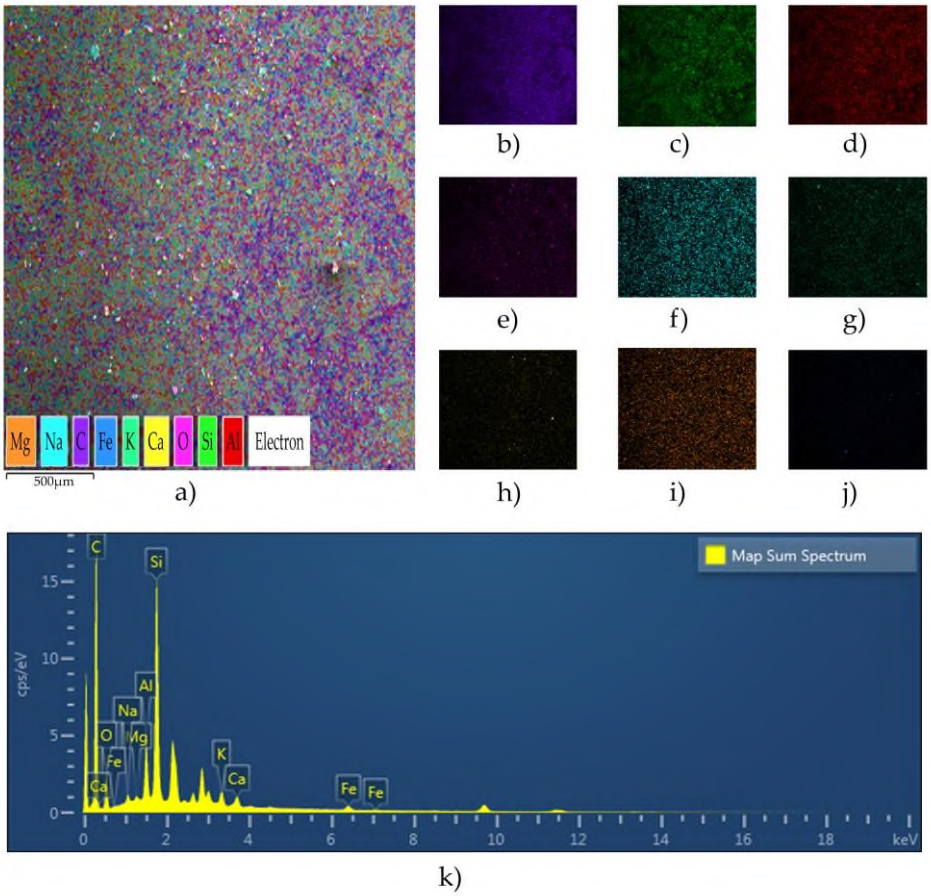

Figure 13. a) Elemental analysis and distribution map of ER/SSP-2 composite, b) Distribution of carbon element in ER/SSP-2 composite, c) Distribution of silicon element in ER/SSP-2 composite, d) Distribution of aluminum element in ER/SSP-2 composite, e) Distribution of oxygen element in ER/SSP-2 composite, f) Distribution of sodium element in ER/SSP-2 composite, g) Distribution of potassium element in ER/SSP-2 composite, h) Distribution of calcium element in ER/SSP-2 composite, i) Distribution of magnesium element in ER/SSP-2 composite, j) Distribution of iron element in ER/SSP-2 composite, k) EDS analysis in ER/SSP-2 composite

EDS analysis of ER/SSP-3 composite is given in Figure 14. When the map distribution of the elements in Figure 14 is examined, it is seen that it is the most dense carbon element. Moreover, the densities and distribution map of the other elements in the ER/SSP-3 composite are oxygen, silicon, aluminum, potassium, iron, calcium, sodium and magnesium, respectively (Figure 14b-14j). It shows that the carbon and oxygen elements belong to the epoxy matrix. However, due to the carbonation of some of the compounds in Sille stone, the carbon element is also found in the stone powder. Oxygen and other elements are also present in the compounds of stone powder. Silicon and oxygen element in ER/SSP-3 composite show an increase compared to ER/SSP-1 and ER/SSP-2. This is due to the decrease in the epoxy matrix due to the increase in the amount of stone powder. According to the results of the EDS analysis of the ER/SSP-3 composite, the agglomeration between the epoxy matrix and the stone powder prevents the homogeneous distribution of the elements. Moreover, this agglomeration causes the formation of pores in the composite material, since it cannot cover the stone powder to the epoxy matrix over the entire area (Figure 14a-14k).

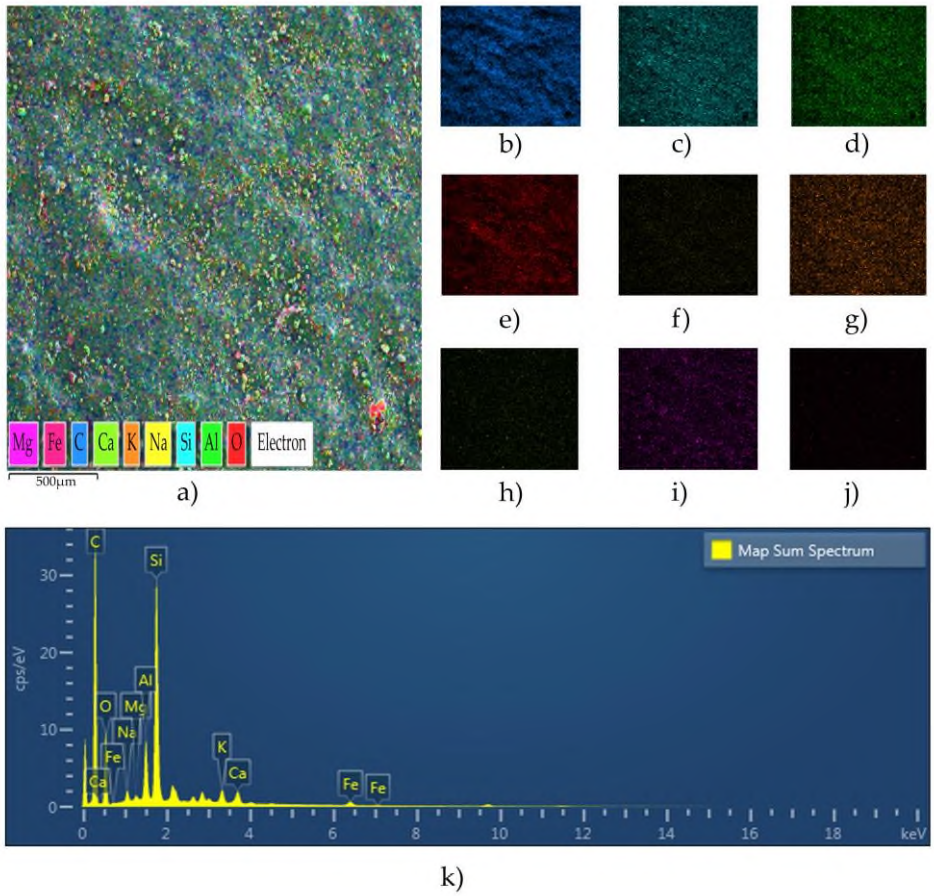

Figure 14. a) Elemental analysis and distribution map of ER/SSP-3 composite, b) Distribution of carbon element in ER/SSP-3 composite, c) Distribution of silicon element in ER/SSP-3 composite, d) Distribution of aluminum element in ER/SSP-3, e) Distribution of oxygen element in ER/SSP-3 composite, f) Distribution of sodium element in ER/SSP-3 composite, g) Distribution of potassium element in ER/SSP-3 composite, h) Distribution of calcium element in ER/SSP-3 composite, i) Distribution of magnesium element in ER/SSP-3 composite, j) Distribution of iron element in ER/SSP-3 composite, k) EDS analysis in ER/SSP-3 composite

EDS analysis of ER/SSP-4 composite is given in Figure 15. When the map distribution of the elements in Figure 15 is examined, it is seen that it is the most dense carbon element. Moreover, the densities and distribution map of the other elements in the ER/SSP-4 composite are oxygen, silicon, aluminum, potassium, iron, calcium, sodium and magnesium, respectively (Figure 15b-15j). It shows that the carbon and oxygen elements belong to the epoxy matrix. However, due to the carbonation of some of the compounds in Sille stone, the carbon element is also found in the stone powder. Oxygen and other elements are also present in the compounds of stone powder. According to the results of the EDS analysis of the ER/SSP-4 composite, the element distribution is more homogeneous than the other composites. Additionally, since the stone powder covers the entire area in the epoxy matrix in the ER/SSP-4 composite, it has been observed that the pores and porosities are less than the other composite types (Figure 15a-15k).

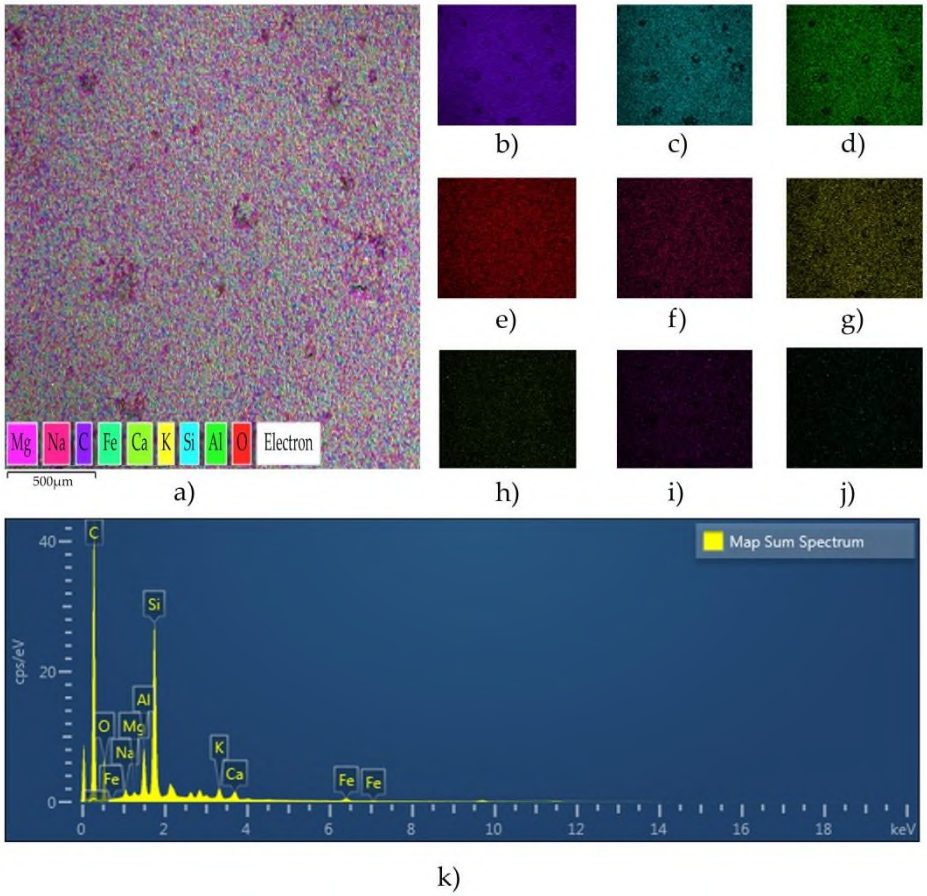

Figure 15. a) Elemental analysis and distribution map of ER/SSP-4 composite, b) Distribution of carbon element in ER/SSP-4 composite, c) Distribution of silicon element in ER/SSP-4 composite, d) Distribution of aluminum element in ER/SSP-4, e) Distribution of oxygen element in ER/SSP-4 composite, f) Distribution of sodium element in ER/SSP-4 composite, g) Distribution of potassium element in ER/SSP-4 composite, h) Distribution of calcium element in ER/SSP-4 composite, i) Distribution of magnesium element in ER/SSP-4 composite, j) Distribution of iron element in ER/SSP-4 composite, k) EDS analysis in ER/SSP-4 composite

3.8. Fourier Transform Infrared Spectroscopy (FTIR)

Infrared electromagnetic waves of ER and ER/SSP composites were made between 4000 and 500 cm^{-1}. Additionally, in the FTIR analysis of the samples, it was applied starting from the 100% transmittance rate from 4000 cm^{-1} wave number to 500 cm^{-1} wave number. While examining the FTIR analysis of the samples, it was observed that the transmittance ratios decreased in the wave number value. The types of bonds corresponding to the vibrations or rotations between the atoms in the sample were determined [51, 52].

FTIR analysis result of ER and ER/SSP composites are given in Table 10 and Figure 16. As can be seen in Table 10 and Figure 16, the peak values at which the transmittance value of ER and ER/SSP composites decreased vary between 3345 cm^{-1} and 554 cm^{-1}. According to the results given in Table 10 shows the O─H stretching the bond type corresponding to the wavenumber peak value at 3345 cm^{-1}, the aliphatic C─H stretching the bond type corresponding to the wavenumber peak value at 2920 cm^{-1}, the C=O strong stretching the bond type corresponding to the wavenumber peak value at 1735 cm^{-1}. Moreover, It also expresses aromatic ring C=C stretching the bond type corresponding to the wavenumber peak value at 1606 cm^{-1}, aromatic C─C stretching the bond type corresponding to the wavenumber peak value at 1541 cm^{-1}, CH_3 in the radikal group C─H asymmetrical bending the bond

type corresponding to the wavenumber peak value at 1457 cm^{-1}. Additionally, It have also been detected C─O bonds stretching the bond type corresponding to the wavenumber peak value at 1235 cm^{-1}, Ar─O─R asymmetrical bending the bond type corresponding to the wavenumber peak value at 1180 cm^{-1}, C–O–C of ethers stretching the bond type corresponding to the wavenumber peak value at 1032 cm^{-1}, C–O–C of oxirane group stretching the bond type corresponding to the wavenumber peak value at 825 cm^{-1} [53, 54].

The C–H aromatic ring bending shows the bond type corresponding to the wavenumber peak value at 728 cm^{-1} and 696 cm^{-1}, and C–H, N–H bending the bond type corresponding to the wavenumber peak value at 554 cm^{-1} [55]. While these results were seen in all samples, a different peak value was determined at 1090 cm^{-1} wave number, unlike the ER samples of ER/SSP composites. It expresses the C–N of ethers aromatic stretching the bond type corresponding to the wavenumber peak value at 1090 cm^{-1} [56]. As a result of the FTIR analysis of the ER/SSP composite samples, the peak value at a wavelength of 1090 cm^{-1} emerged due to the strong C–N bonds between the epoxy matrix and the stone powder.

Table 10. Type of bonds formed between corresponding atoms according to wave numbers of ER and ER/SSP composites

Wavenumber (cm^{-1})	**Bond Type**
3345	O─H stretching
2920	Aliphatic C─H stretching
1735	C=O strong stretching
1606	Aromatic Ring C=C stretching
1541	Aromatic C─C stretching
1457	CH_3 in the radikal group C─H asymmetrical bending
1235	C─O bonds stretching
1180	Ar─O─R asymmetrical bending
1090	C─N aromatic stretching
1032	C–O–C of ethers bonds stretching
825	C–O–C of oxirane group bonds stretching
728	C–H aromatic ring bending
696	C–H aromatic ring bending
554	C–H, N–H bending

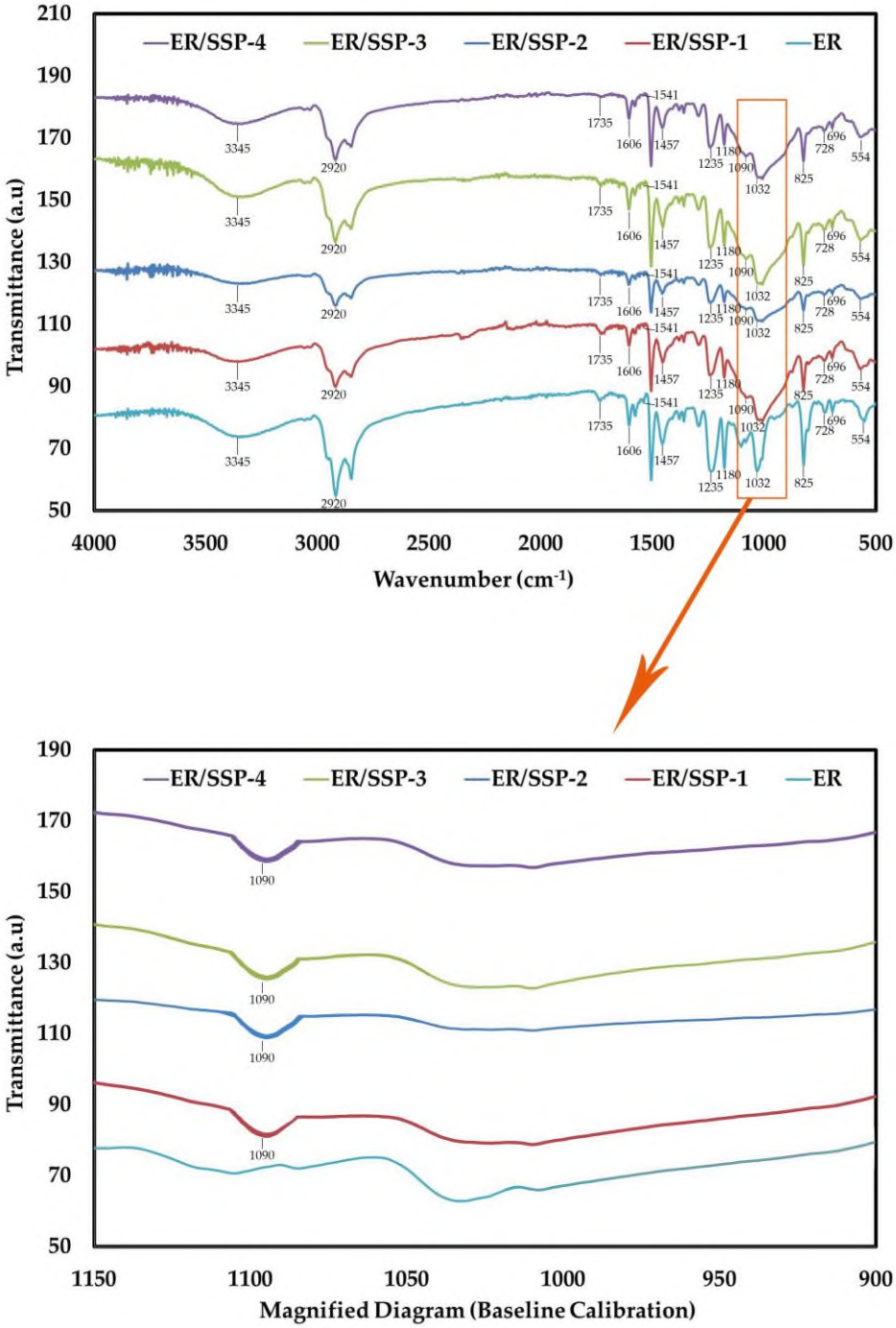

Figure 16. FTIR analysis result graph of ER and ER/SSP composites

4. CONCLUSIONS

In this study, the mechanical, physical and microstructural properties of SSP repair mortar with epoxy matrix were demonstrated. Based on the test results conducted in the study, the following conclusions can be drawn:

- According to the void determination and water absorption test results, it has been determined that the composite mortar has a lower water absorption rate and porosity than Sille stone. The low water absorption rate and pore numbers of the composite material reduce the damage caused by decay in the structure. Moreover, the low water absorption rate of repair mortars in the restoration of cultural assets is beneficial for the protection of the structure.

- Due to the porous structure and high water absorption rate of Sille stone, it causes deterioration and damage in structures such as humidity and flowering.
- According to the test results performed to determine the mechanical properties of the repair mortar, the strength of the ER/SSP-4 composite was found to be higher than the other composite types. Additionally, the use of high levels of SSP in the production of this composite contributes to both the economy of the material and the protection of natural resources and the environment.
- The agglomeration between the ER/SSP-2 and ER/SSP-3 epoxy matrix and the stone powder increased the number of voids and pores in the composites. This reduced the strength of the agglomeration composites.
- According to SEM images, increasing the amount of SSP in ER/SSP composites creates rough surfaces and pores in the material. Moreover, it has been observed that the bond strength between the epoxy matrix and the stone powder has an effect on the loading of stone powder on the composite and the homogeneous distribution of the epoxy matrix.
- SEM-EDS and FTIR analyzes of ER/SSP composites were shown to be compatible with the mechanical test results.

As a result, the high strength, low water absorption rate and pore properties of epoxy matrix composite mortars provide great potential for the restoration applications of historical buildings constructed from Sille stone. Moreover, the color of the epoxy matrix composite mortars being compatible with the color of the sille stone contributes to the preservation of the original forms in the restoration of historical buildings.

Declaration of Ethical Standards

The authors declare that the study complies with all applicable laws and regulations and meets ethical standards.

Credit Authorship Contribution Statement

A.C.A: Investigation, Experimental Section, Data Curation, Methodology, Investigation, Writing – original draft. **M.T:** Validation, Writing -review & editing, Supervision.

Declaration of Competing Interest

The authors declare that they have no known competing financial interests or personal relationships that could have appeared to influence the work reported in this paper.

Funding / Acknowledgements

This study was prepared from the first author's PH.D. thesis. This thesis study was supported by the Scientific Research Projects Commission of the Konya Technical University within the scope of Ph.D. (Project number: 211120045). The authors are grateful for the support provided by Konya Technical University (Türkiye). Experimental studies of this research were carried out in laboratories of the Science and Technology Research and Application Center (BITAM) at Necmettin Erbakan University. We would like to thank the staff of BITAM for their assistance as well.

Data Availability

The data that support the findings of this study are available from the corresponding author upon reasonable request.

REFERENCES

[1] A. Isebaert, L. Van Parys, and V. Cnudde, "Composition and compatibility requirements of mineral repair mortars for stone–A review," *Construction and Building Materials,* vol. 59, pp. 39-50, 2014.

[2] L. Schueremans, Ö. Cizer, E. Janssens, G. Serré, and K. Van Balen, "Characterization of repair mortars for the assessment of their compatibility in restoration projects: Research and practice," *Construction and building materials,* vol. 25, no. 12, pp. 4338-4350, 2011.

[3] J.-D. Mertz, M. Guiavarc'h, and P. Pagnin, "Dilation behaviour of lime mortars for restoration work: application to the compatibility of cracked stone reassembling," *European Journal of Environmental and Civil Engineering,* vol. 16, no. 5, pp. 527-542, 2012.

[4] M. Fener and İ. İnce, "Effects of the freeze–thaw (F–T) cycle on the andesitic rocks (Sille-Konya/Turkey) used in construction building," *Journal of African Earth Sciences,* vol. 109, pp. 96-106, 2015.

[5] M. E. Hatır, "Determining the weathering classification of stone cultural heritage via the analytic hierarchy process and fuzzy inference system," *Journal of Cultural Heritage,* vol. 44, pp. 120-134, 2020.

[6] M. E. Hatır, M. Barstuğan, and I. İnce, "Deep learning-based weathering type recognition in historical stone monuments," *Journal of Cultural Heritage,* vol. 45, pp. 193-203, 2020.

[7] M. Korkanç *et al.*, "Interpreting sulfated crusts on natural building stones using sulfur contour maps and infrared thermography," *Environmental Earth Sciences,* vol. 78, pp. 378, 2019.

[8] A. Ozdemir, "Capillary water absorption potential of some building materials," *Geological Engineering,* vol. 26, no. 1, pp. 19-32, 2002.

[9] V. Zedef, K. Kocak, A. Doyen, H. Ozsen, and B. Kekec, "Effect of salt crystallization on stones of historical buildings and monuments, Konya, Central Turkey," *Building and Environment,* vol. 42, no. 3, pp. 1453-1457, 2007.

[10] Ç. Öztürk, S. Akpınar, and M. Tarhan, "Investigation of the usability of Sille stone as additive in floor tiles," *Journal of the Australian Ceramic Society,* vol. 57, pp. 567-577, 2021.

[11] J. Lanas, J. P. Bernal, M. Bello, and J. A. Galindo, "Mechanical properties of natural hydraulic lime-based mortars," *Cement and concrete research,* vol. 34, no. 12, pp. 2191-2201, 2004.

[12] E. Navrátilová and P. Rovnaníková, "Pozzolanic properties of brick powders and their effect on the properties of modified lime mortars," *Construction and Building Materials,* vol. 120, pp. 530-539, 2016.

[13] Y. Zeng, B. Zhang, and X. Liang, "A case study and mechanism investigation of typical mortars used on ancient architecture in China," *Thermochimica Acta,* vol. 473, no. 1-2, pp. 1-6, 2008.

[14] G. F. Huseien and K. W. Shah, "Performance evaluation of alkali-activated mortars containing industrial wastes as surface repair materials," *Journal of Building Engineering,* vol. 30, p. 101234, 2020.

[15] R. A. Alves, K. Strecker, R. B. Pereira, and T. H. Panzera, "Mixture design applied to the development of composites for steatite historical monuments restoration," *Journal of Cultural Heritage,* vol. 45, pp. 152-159, 2020.

[16] B. Dębska and L. Lichołai, "A study of the effect of corrosive solutions on selected physical properties of modified epoxy mortars," *Construction and Building Materials,* vol. 65, pp. 604-611, 2014.

[17] E. Tesser, L. Lazzarini, and S. Bracci, "Investigation on the chemical structure and ageing transformations of the cycloaliphatic epoxy resin EP2101 used as stone consolidant," *Journal of Cultural Heritage,* vol. 31, pp. 72-82, 2018.

[18] E. M. Alonso-Villar, T. Rivas, and J. S. Pozo-Antonio, "Adhesives applied to granite cultural heritage: effectiveness, harmful effects and reversibility," *Construction and Building Materials,* vol. 223, pp. 951-964, 2019.

[19] J.-L. Roig-Salom, M.-T. Doménech-Carbó, J. de la Cruz-Cañizares, F. Bolívar-Galiano, M.-J. Pelufo-Carbonell, and Y. Peraza-Zurita, "SEM/EDX and vis spectrophotometry study of the stability of resin-bound mortars used for casting replicas and filling missing parts of historic stone fountains," *Analytical and bioanalytical chemistry,* vol. 375, pp. 1176-1181, 2003.

[20] A. C. Ari, M. Tosun, and Y. R. Eker, "Polymer matrix and stone powder based composite mortar for the restoration of sille stone structures," *Studies in Conservation,* vol. 69, no. 1, pp. 50-57, 2024.

[21] F. Güyer *et al.*, "Konya İli Çevre Jeolojisi ve Doğal Kaynaklar," *MTA Rap,* no. 42149, 1998.

[22] A. C. Arı, M. Tosun, İ. Oral, and Y. R. Eker, "Ultrasonic characterization of polymer based sille stone powder composite mortars," *Turkish Journal of Civil Engineering,* vol. 35, no. 3, pp. 21-46, 2024.

[23] ASTM-D2734, *Standard test method for void content of reinforced plastics*, 2009.

[24] URL1. (19.07.2022). Available: https://www.erbakan.edu.tr/bitam/sayfa/3297.

[25] ASTM-D570, *Standard test method for water absorptionof plastics*, 2005.

[26] ASTM-D790, *Standard test methods for flexural properties of unreinforced and reinforced plastics and electrical insulating materials*, 2000.

[27] ASTM-D695, *Standard test method for compressive properties of polymer matrix composite materials*, 2010.

[28] ASTM-D638, *Standard test method for tensile properties of plastic*, 2005.

[29] ASTM-D2240, *Standard test method for rubber property-durometer hardness*, 2010.

[30] J. Lanas and J. I. Alvarez-Galindo, "Masonry repair lime-based mortars: factors affecting the mechanical behavior," *Cement and concrete research,* vol. 33, no. 11, pp. 1867-1876, 2003.

[31] Á. Török and B. Szemerey-Kiss, "Freeze-thaw durability of repair mortars and porous limestone: compatibility issues," *Progress in Earth and Planetary Science,* vol. 6, pp. 42, 2019.

[32] Z. Zheng, Y. Li, X. Ma, X. Zhu, and S. Li, "High density and high strength cement-based mortar by modification with epoxy resin emulsion," *Construction and Building Materials,* vol. 197, pp. 319-330, 2019.

[33] L. Korat, B. Mirtič, A. Mladenovič, A. M. Pranjić, and S. Kramar, "Formulation and microstructural evaluation of tuff repair mortar," *Journal of Cultural Heritage,* vol. 16, no. 5, pp. 705-711, 2015.

[34] M. M. Rahman and M. A. Islam, "Effect of epoxy resin on the intrinsic properties of masonry mortars," *Iranian Polymer Journal,* vol. 21, pp. 621-629, 2012.

[35] V. Rajput, S. K. Somani, A. Agrawal, and V. S. Pagey, "Mechanical properties of epoxy composites filled with micro-sized kota stone dust," *Materials Today: Proceedings,* vol. 47, pp. 2673-2676, 2021.

[36] R. Karthikeyan, R. Girimurugan, G. Sahoo, P. Maheskumar, and A. Ramesh, "Experimental investigations on tensile and flexural properties of epoxy resin matrix waste marble dust and tamarind shell particles reinforced bio-composites," *Materials Today: Proceedings,* vol. 68, pp. 2215-2219, 2022.

[37] M. L. P. Gomes, E. A. Carvalho, L. N. Sobrinho, S. N. Monteiro, R. J. Rodriguez, and C. M. F. Vieira, "Production and characterization of a novel artificial stone using brick residue and quarry dust in epoxy matrix," *Journal of materials research and technology,* vol. 7, no. 4, pp. 492-498, 2018.

[38] K. A. Gour, R. Ramadoss, and T. Selvaraj, "Revamping the traditional air lime mortar using the natural polymer–Areca nut for restoration application," *Construction and Building Materials,* vol. 164, pp. 255-264, 2018.

[39] F. Iucolano, B. Liguori, and C. Colella, "Fibre-reinforced lime-based mortars: A possible resource for ancient masonry restoration," *Construction and Building Materials,* vol. 38, pp. 785-789, 2013.

[40] J. A. V. Gonçalves, D. A. T. Campos, G. d. J. Oliveira, M. d. L. d. S. Rosa, and M. A. Macêdo, "Mechanical properties of epoxy resin based on granite stone powder from the Sergipe fold-and-thrust belt composites," *Materials Research,* vol. 17, no. 4, pp. 878-887, 2014.

[41] M. L. Santarelli, F. Sbardella, M. Zuena, J. Tirillò, and F. Sarasini, "Basalt fiber reinforced natural hydraulic lime mortars: A potential bio-based material for restoration," *Materials & Design,* vol. 63, pp. 398-406, 2014.

[42] B. Kekeç, "Investigation of the texture, physical and mechanical properties of the rocks used as building stone," Seljuk University Graduate School of Natural Sciences, MS Thesis, Konya, 2005.

[43] C. Borsellino, L. Calabrese, and G. Di Bella, "Effects of powder concentration and type of resin on the performance of marble composite structures," *Construction and Building Materials,* vol. 23, no. 5, pp. 1915-1921, 2009.

[44] D. Olmos, A. Aznar, and J. González-Benito, "Kinetic study of the epoxy curing at the silica particles/epoxy interface using the fluorescence of pyrene label," *Polymer testing,* vol. 24, no. 3, pp. 275-283, 2005.

[45] M. A. R. Bhutta, "Effects of polymer–cement ratio and accelerated curing on flexural behavior of hardener-free epoxy-modified mortar panels," *Materials and structures,* vol. 43, pp. 429-439, 2010.

[46] K. Hassan, P. Robery, and L. Al-Alawi, "Effect of hot-dry curing environment on the intrinsic properties of repair materials," *Cement and Concrete Composites,* vol. 22, no. 6, pp. 453-458, 2000.

[47] A. Mallat and A. Alliche, "Mechanical investigation of two fiber-reinforced repair mortars and the repaired system," *Construction and building materials,* vol. 25, no. 4, pp. 1587-1595, 2011.

[48] M. Medeiros, P. Helene, and S. Selmo, "Influence of EVA and acrylate polymers on some mechanical properties of cementitious repair mortars," *Construction and building materials,* vol. 23, no. 7, pp. 2527-2533, 2009.

[49] S.-Y. Fu, X.-Q. Feng, B. Lauke, and Y.-W. Mai, "Effects of particle size, particle/matrix interface adhesion and particle loading on mechanical properties of particulate–polymer composites," *Composites Part B: Engineering,* vol. 39, no. 6, pp. 933-961, 2008.

[50] T. T. L. Doan, H. M. Brodowsky, U. Gohs, and E. Mäder, "Re-use of marble stone powders in producing unsaturated polyester composites," *Advanced Engineering Materials,* vol. 20, no. 7, p. 1701061, 2018.

[51] S. Ramesh, K. H. Leen, K. Kumutha, and A. Arof, "FTIR studies of PVC/PMMA blend based polymer electrolytes," *Spectrochimica Acta Part A: Molecular and Biomolecular Spectroscopy,* vol. 66, no. 4-5, pp. 1237-1242, 2007.

[52] M. R. Reddy, A. Subrahmanyam, M. M. Reddy, J. S. Kumar, V. Kamalaker, and M. J. Reddy, "X-RD, SEM, FT-IR, DSC Studies of Polymer Blend Films of PMMA and PEO," *Materials Today: Proceedings,* vol. 3, no. 10, pp. 3713-3718, 2016.

[53] M. R. M. Hafiezal, A. Khalina, Z. A. Zurina, M. D. M. Azaman, and Z. M. Hanafee, "Thermal and flammability characteristics of blended jatropha bio-epoxy as matrix in carbon fiber–reinforced polymer," *Journal of Composites Science,* vol. 3, no. 1, pp. 6, 2019.

[54] F. Kasim, M. Mahdi, J. Hassan, S. Al-Ani, and S. Kasim, "Preparation and optical properties of CdS/Epoxy nanocomposites," *International Journal of Nanoelectronics and Materials,* vol. 5, pp. 57-66, 2012.

[55] G. Nikolic, S. Zlatkovic, M. Cakic, S. Cakic, C. Lacnjevac, and Z. Rajic, "Fast fourier transform IR characterization of epoxy GY systems crosslinked with aliphatic and cycloaliphatic EH polyamine adducts," *Sensors,* vol. 10, no. 1, pp. 684-696, 2010.

[56] A. Carrillo-Castillo and J. G. Osuna-Alarcón, "Preparation and characterization of hybrid materials of epoxy resin type bisphenol a with silicon and titanium oxides by sol gel process," *Journal of the Mexican Chemical Society,* vol. 55, no. 4, pp. 233-237, 2011.